

ASSESSMENT OF AIRCREW RADIATION EXPOSURE BY FURTHER MEASUREMENTS AND MODEL DEVELOPMENT

B. J. Lewis^{1,*}, M. Desormeaux¹, A. R. Green¹, L. G. I. Bennett¹, A. Butler¹, M. McCall¹ and J. C. Saez Vergara²

¹Department of Chemistry and Chemical Engineering, Royal Military College of Canada, P.O. Box 17000, Kingston, Ontario, Canada K7K 7B4

²Centro de Investigaciones Energéticas, Medioambientales y Tecnológicas (CIEMAT), Av. Complutense 22, E-28040 Madrid, Spain

Received March 26 2004, amended May 5 2004, accepted May 6 2004

A methodology is presented for collecting and analysing exposure measurements from galactic cosmic radiation using a portable equipment suite and encapsulating these data into a semi-empirical model/Predictive Code for Aircrew Radiation Exposure (PCAIRE) for the assessment of aircrew radiation exposure on any flight over the solar cycle. The PCAIRE code has been validated against integral route dose measurements at commercial aircraft altitudes during experimental flights made by various research groups over the past 5 y with code predictions typically within $\pm 20\%$ of the measured data. An empirical correlation, based on ground-level neutron monitoring data, is detailed further for estimation of aircrew exposure from solar particle events. The semi-empirical models have been applied to predict the annual and career exposure of a flight crew member using actual flight roster data, accounting for contributions from galactic radiation and several solar energetic-particle events over the period 1973–2002.

INTRODUCTION

The natural background radiation field is enhanced at jet aircraft altitudes (~ 6.1 – 18 km) due to interaction of primary galactic cosmic ray (GCR) particles with the Earth's atmosphere. The GCR primary particles, consisting of $\sim 90\%$ protons, 9% alpha particles and 1% heavy nuclei (ranging from carbon to iron), result from supernova explosions and active galactic nuclei^(1,2). These particles are accelerated during their interstellar migration where their energy spectrum follows approximately a power law of the form $E^{-2.7}$ above ~ 1 GeV up to 10^{15} eV, and E^{-3} above this latter energy as they enter into the solar magnetic field. The fluence rate is fairly constant in time and approaches the Earth in an isotropic fashion.

The penetrating ability of these ionised particles from outside the solar system is directly affected by their magnetic rigidity, leading to a $\sim 40\%$ variation of the dose rate over the solar cycle. The galactic radiation contribution is at a maximum during solar minimum conditions due to a decreased solar modulation. The primary cosmic rays are also affected by the magnetic field of the Earth, where those particles that enter near the poles experience little deflection, while those entering near the equator approach at right angles so that they are deflected if their rigidity is below the geomagnetic cut-off rigidity. Hence, the galactic radiation exposure varies with latitude where the dose rate is about two to three times

greater nearer the poles compared to that at the equatorial regions. Finally, those particles that enter into the upper layers of the atmosphere interact with atmospheric nuclei that results in a cascade of secondary particles (i.e. protons, neutrons, and π and K mesons). The charged mesons decay radioactively into muons that provide the greatest contribution to the ground-level exposure. Electromagnetic showers are also produced as the muons further decay into electrons and neutrinos, while the neutral pions decay into photons. The build-up of these secondary particles competes with their attenuation in the atmosphere so that the dose rate also varies with altitude in which a maximum is reached at the so-called 'Pfozter' maximum at ~ 20 km above sea level. In summary, the aircrew radiation exposure from galactic cosmic radiation varies with the date (i.e. solar cycle period), geomagnetic latitude and altitude of the flight.

Additional exposure to aircrew may also occur from high-energy solar particles produced in association with solar flares and coronal mass ejections (CMEs). This additional exposure becomes more important at higher (i.e. supersonic) jet altitudes and at latitudes close to the magnetic poles, especially with the occurrence of a ground level event (GLE). Magnetic energy release from the sun can send a large number of charged particles (mainly protons, some alpha particles and a few heavier nuclei) into the atmosphere with maximum energies between ~ 10 and 700 MeV. In the largest solar energetic-particle (SEP) events, particle acceleration results via shock waves that are driven out of the sun

*Corresponding author: lewis-b@rmc.ca

with CMEs where protons near the Earth can reach energies up to and above ~ 1 GeV^(3,4). The intensity of these particle fluence rates and their spectra are highly variable where the SEP events follow an ~ 80 – 100 y Gleissberg cycle. The sunspots are more predominant during solar maximum conditions, and the reconnection of the sunspot magnetic fields frequently result in CMEs. The energy of these solar protons, however, is much less than that of particles of galactic origin.

As a result of the recommendations by the International Commission on Radiological Protection (ICRP) made in 1990⁽⁵⁾, aircrew in the European Union (EU) and Canada have been classified as occupationally exposed to cosmic radiation^(6–9). In fact, the EU Directive has already been incorporated into laws and regulations of the majority of the EU Member States. It has been included as well in the aviation safety standards and procedures of the Joint Aviation Authorities. In Canada, an advisory circular by Transport Canada has been issued to suggest voluntary action to manage such exposures to a level < 6 mSv y^{-1} ⁽⁹⁾. These regulations present unique challenges to the airline industry as the conventional dosimetric approach of monitoring individuals would be both costly and difficult to manage. Alternatively, since the aircrew exposure on a given route is relatively constant (i.e. within the solar cycle variation), this exposure can be predicted based on theoretical and/or experimental knowledge of the route dose. In fact, following guidance from the European Commission and the ICRP⁽¹⁰⁾, the preferred method for assessment of aircraft crew exposure in both the EU and Canada is by computation. This method relies on staff roster information and flight profiles with the use of dose rate calculations, which can be derived from either theoretical models or empirical correlations as a function of altitude, geomagnetic latitude and solar modulation⁽¹¹⁾. Such calculations, however, are to be verified periodically by measurements.

Consequently, over the past decade, with the recommendation of the ICRP 60, there has been a significant effort to measure the aircrew radiation exposure^(12–23). Moreover, theoretical treatments have further been developed concurrently to calculate this exposure from particle-transport theory through the atmosphere. For instance, Monte Carlo analysis with the FLUKA code^(24–26) has led to the aircrew exposure tool EPCARD⁽²⁷⁾. Similarly, a deterministic solution of the Boltzmann transport equation via the LUIN code^(28,29) has provided the basis for the CARI aircrew-exposure code⁽³⁰⁾. Moreover, extensive measurements have led to a correlational model implemented in the PCAIRE code for aircrew exposure assessment⁽³¹⁾. These simple calculational tools can then be used to manage the aircrew route exposure in light of regulatory requirements.

In the current work, ambient dose equivalent rates have been measured with a variety of portable equipment at the Royal Military College (RMC) (e.g., tissue equivalent proportional counter (TEPC), extended-range neutron remmeter, ionisation chamber, silicon-based LIULIN spectrometer, neutron bubble detectors and thermoluminescence dosimeters) in 122 scientific measurement flights, which spanned the entire cut-off rigidity potential of the Earth's magnetic field over the current solar cycle from 1999 to 2003. Using some of these data, an empirical correlation has been developed to allow for the interpolation of the ambient dose equivalent rate for any global position, altitude and date. Based on this analysis, a Predictive Code for Aircrew Radiation Exposure (PCAIRE) has been developed to provide a dose prediction for any given flight route⁽²²⁾. A correlation has been developed further to account for spurious exposures from solar particle events (i.e. based on a post-event analysis of ground-level neutron monitor data). The further development of the PCAIRE model and its validation with the latest measurements is detailed in this paper.

EXPERIMENTAL PROCEDURES

Radiation exposure levels were measured on-board various flights with a Far West HAWK TEPC. The TEPC is capable of detecting both low-linear energy transfer (LET) and high-LET particles. This instrument provides a determination of the absorbed dose by employing a large (12.7 cm diameter) low-density cavity to simulate a microscopic volume of tissue of equal atomic composition (i.e. a 2- μ m diameter tissue site). The Far West HAWK TEPC was designed for portability and simplicity in airline flight measurements. It consists of a grounded anode type spherical-walled detector (LET-SW-5) with an attached preamplifier and spectrometer box that stores full data spectra each minute on a non-volatile flash memory card. The instrument, in its carry-on case, is placed in the aircraft cabin and is powered by four standard 'D' cells for up to five days of operation. The in-flight operation of the TEPC requires only that the power be switched on before takeoff and switched off after landing. The raw binary data stored on the flash memory card during the flight are then downloaded at a later date to a computer. Custom software is used to convert the raw binary data to spectral results that were stored as text files. A description of the microdosimetric analysis is given in Ref. (15). The TEPC provides a spectral measurement of the lineal energy, y , where a quality factor is required so that the absorbed dose distribution can be related to the operational quantity of ambient dose equivalent $H^*(10)$. Although a relationship for the quality factor as a function of y , $Q(y)$, has been proposed by the International

Commission on Radiation Units and Measurements (ICRU)^(32,33), this methodology has not been sanctioned by the ICRP for radiation protection purposes. Instead, a recommendation is given for the quality factor that depends on the LET (LET or L)⁽⁵⁾. However, the measured ambient dose equivalent rate at altitude differs by <3 % using the two different relationships, when y is employed as a surrogate for L in the ICRP-60 $Q(L)$ function as opposed to the ICRU-40 $Q(y)$ relation⁽¹⁵⁾. As such, the ICRP $Q(L)$ relation is adopted in the current analysis where y is specifically set equal to L , this same approach has been used elsewhere^(13–17,20–23). Minute-by-minute data recorded by the TEPC are correlated to the aircraft's geographical position and altitude using either information obtained by a Global Positioning System (GPS) incorporated directly into the HAWK TEPC, or information provided by the pilot from the flight deck. The data are then averaged over a 30-min period to improve the statistics.

Different types of active detectors were also used on 32 scientific flights in 2002 to measure the individual low-LET (ionising) and high-LET (neutron) components of the mixed-radiation field (which can be appropriately summed for comparison to the TEPC results). The various portable active instruments discussed in this study, include (i) a battery-powered Eberline FHT 191 N high-pressure ionisation chamber (IC); and (ii) a battery-powered extended-range neutron detector (SWENDI-II)

(consisting of an E-600 Smart portable radiation monitor and Wide Energy Neutron Detection Instrument (WENDI-II)). The ionisation chamber is operated with a nitrogen and inert gas mixture at a pressure of 0.7 MPa. For photons of energy 40 keV to 7 MeV, and dose rates between 10 nSv h^{-1} and 10 Sv h^{-1} , the dose uncertainties were <10% based on a ^{137}Cs calibration. The WENDI-II contains a tungsten powder fill to improve its response to high-energy neutrons. In particular, this detector provides an improved response for 10 MeV to 5 GeV neutrons as compared with popular commercial remmeters (e.g. the Eberline–Hankins–NRD and Andersson–Braun)⁽³⁴⁾.

As shown in Solar modulation and latitude effects section, the summed results are reasonably consistent with that of the TEPC, providing further confidence in the use of the more complete TEPC dataset for model development.

Equipment calibration

An older version of the TEPC was used for the measurements made in 1999. This original TEPC was calibrated at the Physikalisch Technische Bundesanstalt (PTB) in 2000, where it was shown that it would systematically overpredict by ~10% in a ^{137}Cs gamma field, ~13% when exposed to monoenergetic neutrons (0.565–14.8 MeV) (Figure 1), and ~19% in polyenergetic neutron fields from ^{252}Cf and Am–Be sources. Consequently, a constant calibration

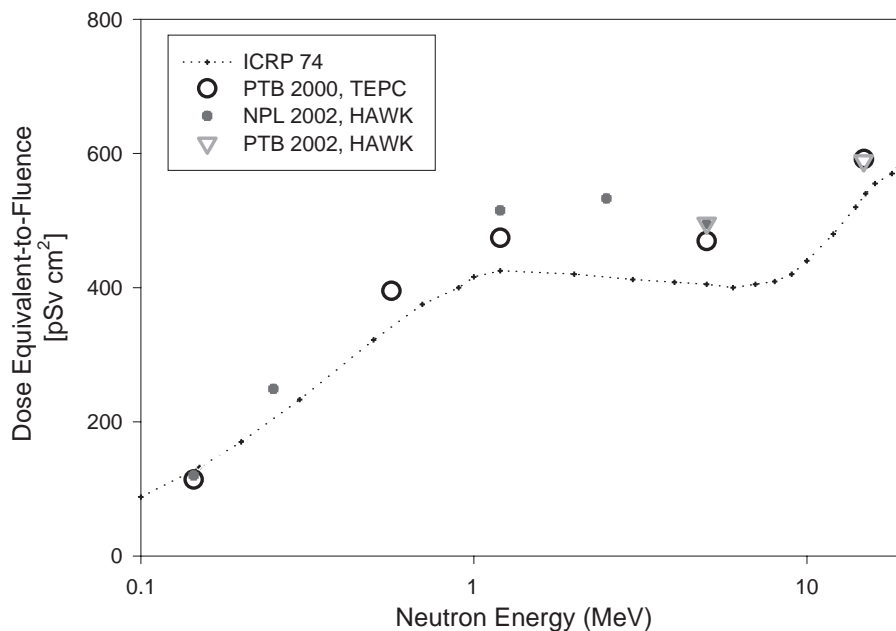


Figure 1. TEPC results using monoenergetic neutrons and comparison to ICRP-74.

factor of $f = 1/1.15 = 0.87$ was applied to the TEPC measurements (H_{TEPC}) in order to convert these data into an ambient dose equivalent $H^*(10)$ where:

$$H^*(10) = fH_{\text{TEPC}}. \quad (1)$$

Following the upgrade of the TEPC to a HAWK version for the measurement campaign in 2002–2003, further calibration testing was performed in 2002 at the PTB and the National Physics Laboratory (NPL) (Figure 1). While the new HAWK was still overresponsive, the offset between the low-LET and the high-LET radiation fields was too large to be approximated by a simple constant (Table 1 and

Table 1. Calibration test results for polyenergetic neutrons and gamma radiation fields.

Field	Known $H^*(10)$ rate ($\mu\text{Sv h}^{-1}$)	2002 HAWK measured $H^*(10)$ rate ($\mu\text{Sv h}^{-1}$)	2002 HAWK % difference ^c
²⁵² Cf	66.3 ^a	86.5 ^{a,b}	30.5
¹³⁷ Cs	40.0	41.9	4.8
¹³⁷ Cs	10.0	10.5	5.5

^aExposure corrected for backscattering using a shadow cone.

^bFiltered radiation with $y > 10 \text{ keV } \mu\text{m}^{-1}$ (no gamma radiation).

^c% Difference = (Measured – Known)/Known \times 100.

Figure 1). The under-prediction for low-energy neutrons in Figure 1 at 0.144 MeV results since the recoil protons have a transport path length that is smaller than the simulated diameter of 2 μm . Overall, the difference between the observed HAWK ambient dose equivalent-to-fluence ratio (H_{TEPC}/Φ) and the ICRP-74 Ref. (35) was found to be $\sim 25\%$ for neutrons (i.e. for polyenergetic and monoenergetic neutrons between 0.25 and 5 MeV) and $\sim 5\%$ for gamma radiation.

Thus, on consideration of the calibration results in Table 1 and Figure 1, and because the neutron composition varies with latitude at jet altitudes, the following calibration factor, f , was employed for Equation 1 for the mixed-field measurement at aircraft altitudes:

$$f = \frac{1}{1 + f_n \times 0.25 + (1 - f_n) \times 0.05}, \quad (2)$$

where f_n is the fraction of the neutron composition (in units of ambient dose equivalent) of the mixed-LET field. The neutron fraction, f_n , can be determined experimentally by comparing the SWENDI measurements (see Ion chamber and extended range neutron remmeter analysis section) to the combined IC plus SWENDI measurements in 2001–2002 as a function of the vertical cut-off rigidity R_c (GV) of the Earth’s magnetic field as shown in Figure 2, where:

$$f_n = 0.484 - 0.0119 \times R_c \quad (3)$$

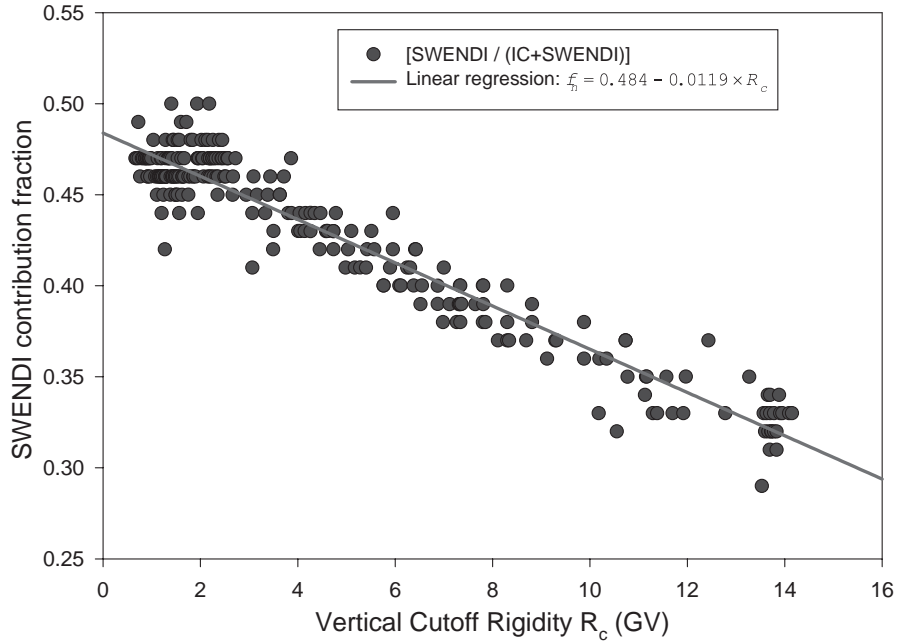


Figure 2. Percentage contribution of neutron field with respect to vertical cut-off rigidity R_c .

In fact, the observed neutron contributions of $\sim 50\%$ at the poles (where $R_c \sim 0$ GV) and $\sim 30\%$ at the equator (where $R_c \sim 15$ GV) are consistent with the theoretical predictions of the FLUKA/EPCARD code⁽²⁷⁾.

Alternatively, the Hawk TEPC can provide from the microdosimetric spectrum an estimate of the low-LET contribution (i.e. ionising component) (for $y < 10$ keV μm^{-1}) and high-LET contribution (i.e. 'neutron' component) (for $y \geq 10$ keV μm^{-1}) of the measured ambient dose equivalent. Thus, the H_{TEPC} value can be equivalently corrected to an $H^*(10)$ value as:

$$H^*(10) = \frac{H_{\text{TEPC}}(y < 10 \text{ keV } \mu\text{m}^{-1})}{1.05} + \frac{H_{\text{TEPC}} - H_{\text{TEPC}}(y < 10 \text{ keV } \mu\text{m}^{-1})}{1.25} \quad (4)$$

Equation 4 is analogous to Equations 1–3. A comparison of these two approaches reveals that either method produces similar ambient dose equivalent rates typically within $\sim 2\%$.

For the current analysis, however, the calibration factor of Equations 2 and 3 is used for the HAWK TEPC in place of a simple constant value ($f = 1/1.15 = 0.87$), as employed for the earlier version of the instrument. This improved calibration factor varies between 0.87 at $R_c = 0$ GV and 0.90 at $R_c = 17$ GV.

MODEL DEVELOPMENT

Altitude effect

The ambient dose equivalent rate data at a given atmospheric depth, h (in g cm^{-2}), can be normalised to an altitude of 10.7 km (or atmospheric depth of $h_o = 243$ g cm^{-2}) using the following relationship⁽²²⁾:

$$f_{\text{Alt}}(h) = e^{-\xi_s(h-h_o)} \left[\frac{1 - e^{-(k_o - \xi_s)h}}{1 - e^{-(k_o - \xi_s)h_o}} \right] + \frac{k_o - \xi_s}{\beta k_o} \left[\frac{e^{-k_o h}}{e^{-\xi_s h_o} - e^{-k_o h_o}} \right] \quad (5)$$

where $\beta \sim 3$ is an effective proportionality constant for the production of secondary particles from primary-particle interactions as determined from balloon-borne flights. The parameter $k_o \sim 0.016$ cm^2 g^{-1} accounts for the attenuation of primary particles in the atmosphere, and is fitted to transport code calculations in order to provide a maximum value of the function in Equation 5 at the Pftzer maximum, where the radiation levels in the atmosphere are observed to reach a maximum due to secondary-particle build-up^(36,37).

In Equation 5, ξ_s is the effective relaxation length for the given particles in the atmosphere, which is a function of the vertical cut-off rigidity,

R_c (in GV). Summed ambient dose equivalents from a lead-modified neutron rem counter (NMX) and an ionisation chamber from a PTB study have been used to develop the following correlations⁽¹⁷⁾:

$$\xi_s = \begin{cases} 0.0085 \text{ cm}^2 \text{ g}^{-1}, & R_c < 4 \text{ GV.} \\ -4.71 \times 10^{-4} R_c + 0.0104, & 4 \text{ GV} \leq R_c \leq 11 \text{ GV.} \\ 0.0052 \text{ cm}^2 \text{ g}^{-1}, & R_c > 11 \text{ GV.} \end{cases} \quad (6)$$

Equation 5 cannot be extrapolated (i.e. in a simple exponential fashion) to lower altitudes because Equation 6 does not reflect the lengthening of the relaxation length due to the muon component that dominates the radiation field closer to the Earth's surface⁽²⁾. Hence, to account for this effect, the relaxation length, ξ_s , can be modified further for low altitudes as derived from data obtained below 7.62 km in 1999, where

$$\xi_{s, \text{LowAlt}} = \begin{cases} 0.650 \xi_s, & A < 4.57 \text{ km} \\ [0.639 + 5.17 \times 10^{-5} \exp(1.16A)] \xi_s, & 4.57 \text{ km} \leq A \leq 7.62 \text{ km} \end{cases}$$

and A is the pressure altitude (in km). The inclusion of this revised model in the code has resulted in improved agreement with measurements made on-board short-haul flights (<2 h of flight time) that are typically at low altitudes.

Solar modulation and latitude effects

TEPC analysis

Cosmic ray intensities vary in a manner that is anti-coincident with solar activity so that galactic radiation is at a maximum during solar minimum conditions. Previous RMC TEPC data were obtained in a period from 1999 (i.e. at a period just past the solar minimum) until 2003 (i.e. in a more active portion of the solar cycle). These two sets of data thus provide an excellent opportunity to determine experimentally the effect of solar modulation on the ambient dose equivalent rate. As mentioned, the measured ambient dose equivalent rates were summed over 30 min intervals to reduce the relative error in the data to $\sim 20\%$. When correlated to the given positional information, these points spanned the full cut-off rigidity of the Earth's magnetic field.

The two sets of data were normalized to an altitude of 10.7 km (or atmospheric depth of $h_o = 243$ g cm^{-2}) using Equation 5. Plotting these data against the vertical cut-off rigidity R_c (which is

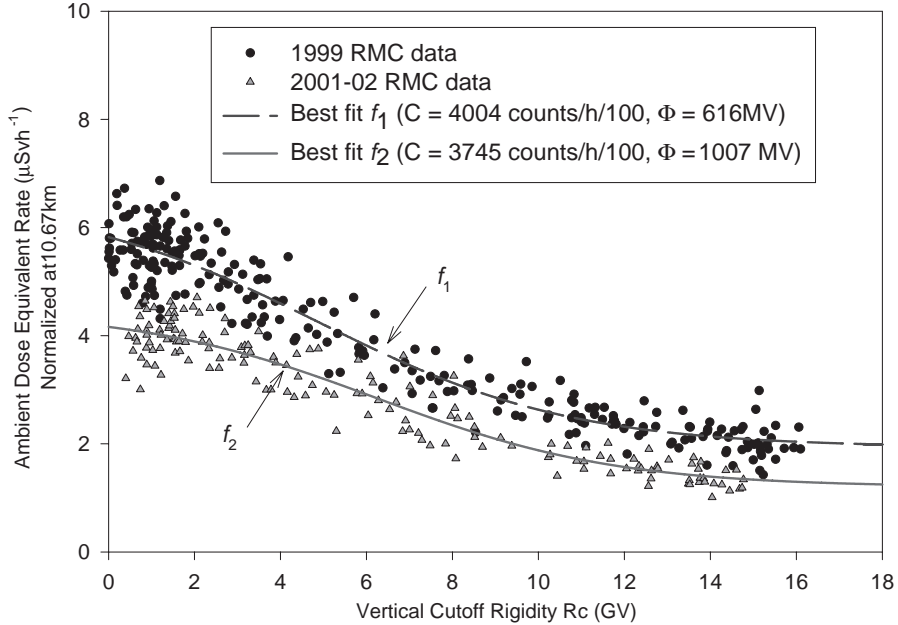


Figure 3. Comparison of ambient dose equivalent rate data measured over the solar cycle.

Table 2. Fitting parameters for data in Figure 3.

Fitting parameters	Dose rate function	
	$f_1(i = 1)$	$f_2(i = 2)$
a_i	1.93	1.20
b_i	4.64	3.27
c_i	4.88	6.26
d_i	2.96	2.79

derived for a given geographical altitude and longitude using the International Geomagnetic Reference Field, IGRF-1995) yields Figure 3. A correlation of the global dose rate as a function of R_c is therefore possible for a given global position for different periods within the solar cycle. A best-fit polynomial to the data in Figure 3 provides the normalised dose rate f_i (in $\mu\text{Sv h}^{-1}$) (at 10.7 km) as a function of R_c (in GV):

$$f_i = a_i + \frac{b_i}{1 + \exp\left[\frac{(R_c - c_i)}{d_i}\right]} \quad (8)$$

The fitting parameters a_i , b_i , c_i and d_i are given in Table 2.

As expected, the dose rate during solar minimum conditions is greater than that during solar maximum ($f_1 > f_2$) due to the effect of solar

modulation. This effect can be modelled by correlating f_1 and f_2 to a given solar modulation parameter as described by one of two available models, i.e. (i) the heliocentric potential model of O'Brien⁽³⁸⁾, which is characterised by a heliocentric potential U (in MV) that is tabulated by the Federal Aviation Administration (FAA) from ground-level neutron monitoring⁽³⁹⁾ and (ii) a diffusion-convection model developed by the National Aeronautics and Space Administration (NASA)—Johnson Space Centre (JSC)⁽⁴⁰⁾, in which the solar modulation strength is determined by a comparable deceleration parameter, Φ (in MV), that depends upon the Climax neutron-monitor count rate. These models are required to determine environmental conditions at the top of the atmosphere, which are specifically needed as boundary conditions by transport codes in order to calculate the propagation of the particle fluence rates (and dose rates) through the atmosphere.

Unfortunately, heliocentric potential values from the original model developer are now proprietary⁽⁴¹⁾. In addition, the NASA-JSC model is a prescriptive model that considers the GCR variations ~ 95 d in advance. This model is primarily intended to provide a prospective estimate of the astronaut-mission exposure (averaged over a one-month period). Hence, its application for route dose estimation of aircrew over a single day is less certain. In particular, it cannot specifically account for daily variations due to solar storm interferences on Earth, such

as ‘Forbush effects’ (where there is a local temporal reduction of the GCR exposure due to a changing magnetic field during a solar event)^(42,43).

Consequently, a new solar modulation model is proposed in this work to address these shortcomings. Since PCAIRE is a semi-empirical model, one can simply correlate the f_1 and f_2 curves in Figure 3 directly to ground-level neutron count rate data C (in counts h^{-1} divided by 100), e.g. at the Climax, neutron monitor (NM) in Colorado (USA)^(44,45). Count rate data at this monitor are in fact also used for the NASA–JSC model. Hence, for the PCAIRE model, either the NASA–JSC deceleration parameter (Φ) or the Climax count rates per 100 (C) are used to describe the effect of solar modulation (i.e. as selected by the user—see PCAIRE code development section). The EPCARD code also employs the NASA–JSC model. Hence, the two curves in Figure 3 are related to the solar modulation parameters (averaged over the given measurement period). Based on comparisons of PCAIRE predictions to experimental data measured as part of the ACREM project during solar minimum conditions⁽⁴⁶⁾, it became apparent that the f_1 curve provided a solar-minimum ‘boundary’ for all values of $C > 4004$ count/h/100 or $\Phi < 616$ MV (Figure 4a). Similarly, the f_2 boundary provides a solar-maximum ‘boundary’ for all values of $C < 3745$ count/h/100 or $\Phi > 1007$ MV, as seen with a comparison to predictions with the EPCARD code (Figure 4b)⁽²⁷⁾. Thus, in the current model, no extrapolation is considered beyond the f_1 and f_2 boundary curves. At other points in the solar cycle, a simple linear interpolation is implemented using Lagrange polynomials. Thus, the effect of the solar cycle on the ambient dose equivalent rate (in $\mu\text{Sv h}^{-1}$) can be

described by:

$$\dot{H}_o^{C \text{ lim } ax} = \begin{cases} f_1 & C > 4004 \text{ count/h/100} \\ \frac{f_1 - f_2}{259}(C - 4004) + f_1, & 3745 \text{ count h/100} \leq C \leq 4004 \text{ count/h/100,} \\ f_2, & 3745 \text{ count/h/100,} \end{cases} \quad (9a)$$

$$\dot{H}_o^\Phi = \begin{cases} f_1, & \Phi < 616 \text{ MV,} \\ \frac{f_2 - f_1}{391}(\Phi - 616) + f_1, & 616 \text{ MV} \leq \Phi \leq 1007 \text{ MV,} \\ f_2, & \Phi > 1007 \text{ MV,} \end{cases} \quad (9b)$$

where f_1 and f_2 are dependent on the cut-off rigidity as detailed in Equation 8. As other data become available over future solar cycles, these data will permit the selection of the better solar modulation model.

Equation 9 therefore provides the basis for the development of a code (see PCAIRE code development section) to allow for ambient dose equivalent rate prediction for any global position and period in the solar cycle (with an appropriate solar modulation model choice). The effect of altitude can be described by Equation 5 so that it can be written generally:

$$\dot{H}(R_c, h; C, \Phi) = \dot{H}_o^{C \text{ or } \Phi} \cdot f_{Alt} \quad (10)$$

Thus, Equation 10 provides an ambient dose equivalent rate prediction at any geographic position (or cut-off rigidity), altitude (up to ~ 20 km) and period in the solar cycle. The ambient dose equivalent rate from Equation 10 can then be suitably integrated over a given route for a dose prediction using either a great circle route or waypoints for the flight⁽²²⁾.

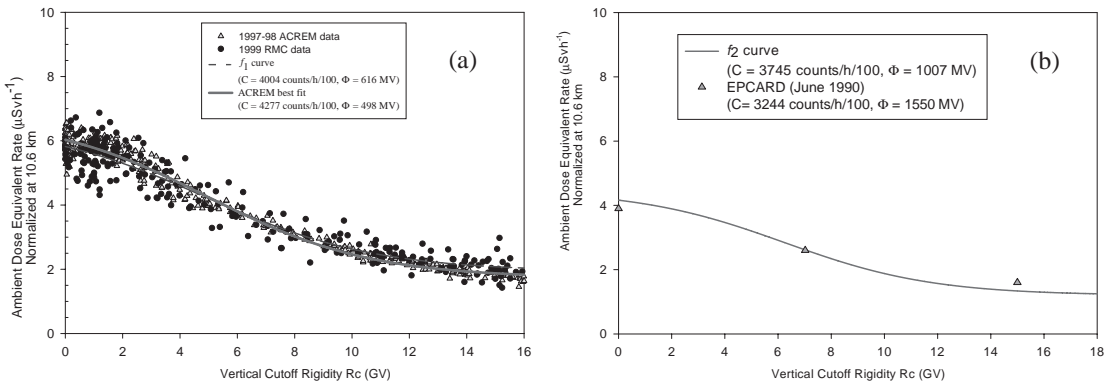


Figure 4. Comparison of the f_1 and f_2 curves with (a) ACREM measurements and (b) EPCARD code predictions for periods at solar minimum and maximum, respectively.

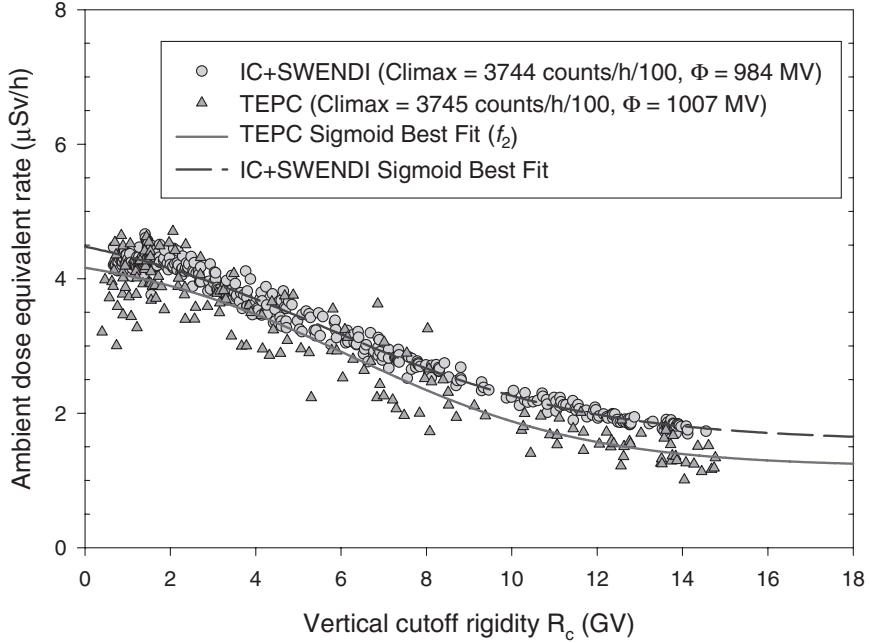


Figure 5. Comparison of ambient dose equivalent rate measurements between the HAWK TEPC and the sum of the IC and SWENDI (for ‘solar maximum’ conditions).

The ambient dose equivalent accumulated during ascent, H_a , and descent, H_d , can be calculated according to:

$$H_{a,d} = \dot{H}_{t_f}^{C \text{ or } \Phi} \cdot \left(\frac{t_{a,d}}{2} \right), \quad (11)$$

where t_a (in s) is the ascent time and t_d (in s) is the descent time. Here $\dot{H}_t^{C \text{ or } \Phi}$ indicates the ambient dose equivalent rate calculated from Equation 10 at the initial altitude over the originating airport and $\dot{H}_f^{C \text{ or } \Phi}$ indicates the ambient dose equivalent rate at the final altitude over the destination airport. The H_a and H_d are added to the at-altitude value in order to provide an output of the ambient dose equivalent for the total flight. Using appropriate conversion factors of effective dose to ambient dose equivalent, $E/H^*(10)$, Equation 10 can be further multiplied by a scaling ratio $fE/H^*(10)$ in order to convert it into an effective dose rate (see Equations 10a and 10b in Ref. (22)).

Ion chamber and extended range neutron remmeter analysis

Using a similar methodology as discussed in the previous section, IC and SWENDI measurements from the 2001–2002 flights were analysed and compared against the TEPC results. As well, IC and NMX data collected in the ACREM investigation in 1997–1998 were also analysed.

A comparison of the IC plus SWENDI data versus the TEPC results is shown in Figure 5 for the same solar maximum period in the solar cycle. There appears to be a deterministic discrepancy, which becomes more pronounced towards the equator ($R_c \sim 16$ GV) (see discussion below). The IC and SWENDI curve (for conditions near solar maximum) was also compared with combined IC and NMX measurements obtained in the ACREM study (during the last solar minimum). As demonstrated in Figure 6a, the two curves approach each other at the equator, where magnetic filtering of the lower energy particles is more significant. This effect is indeed predicted with transport code calculations⁽²⁶⁾.

Figure 6b further shows the comparative results from both the TEPC (Figure 3) and summed instruments (Figure 6a), including an average of the resulting curves for f_1 and f_2 , respectively, by averaging the TEPC and summed instrument results for the given solar modulation condition. Since both the IC and NMX/SWENDI have a response to protons, there may be some double counting that would result in an overestimation of the dose rate curve by simply summing these instruments. On the other hand, the IC is referenced to a photon-equivalent field and therefore this measurement does not take into account an enhanced quality factor for ionising particles

ASSESSMENT OF AIRCREW RADIATION EXPOSURE

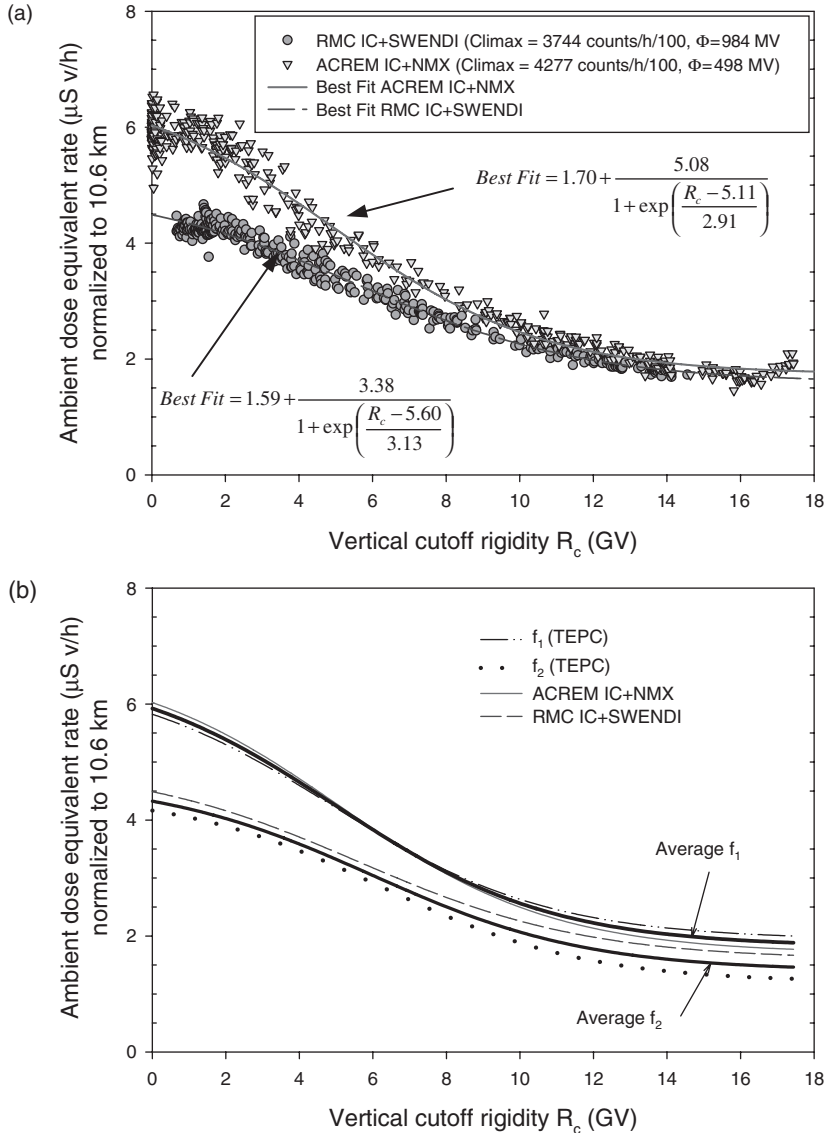
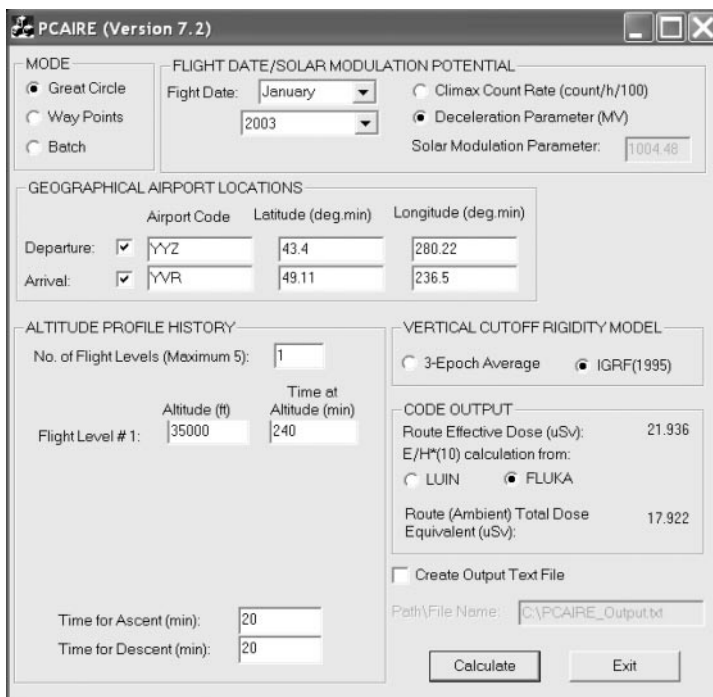


Figure 6. (a) Comparison between combined RMC IC + SWENDI (2001–2002) and ACREM IC + NMX (1997–1998) data (normalised to 10.7 km). (b) Comparison of TEPC and summed instrument (i.e. IC + SWENDI and IC + NMX) curves over the solar cycle. Their averages are depicted in the Average f_1 and f_2 curves (for the given solar modulation condition).

(such as protons) with $\text{LET} > 10 \text{ keV } \mu\text{m}^{-1}$. However, this underestimation may be compensated by the response of the SWENDI to the higher energy protons. In contrast, a Monte Carlo analysis has shown that the response of the TEPC instrument can miss up to $\sim 25\%$ of the (low-LET) ambient dose equivalent due to electronic limitations in the first few channels of the pulse height spectrum if no correction is applied⁽⁴⁷⁾. Hence, a correction

was considered for the first TEPC instrument by simply assuming a constant extrapolated value using the maximum number of counts in the higher channels in order to account for the missing values in the first few channels (which would result in an upper-bound correction). As an improvement to this procedure for the Hawk microdosimetric analysis, an assumed ^{60}Co response curve was applied to these lower channels, although inevitably some

(a)



(b)

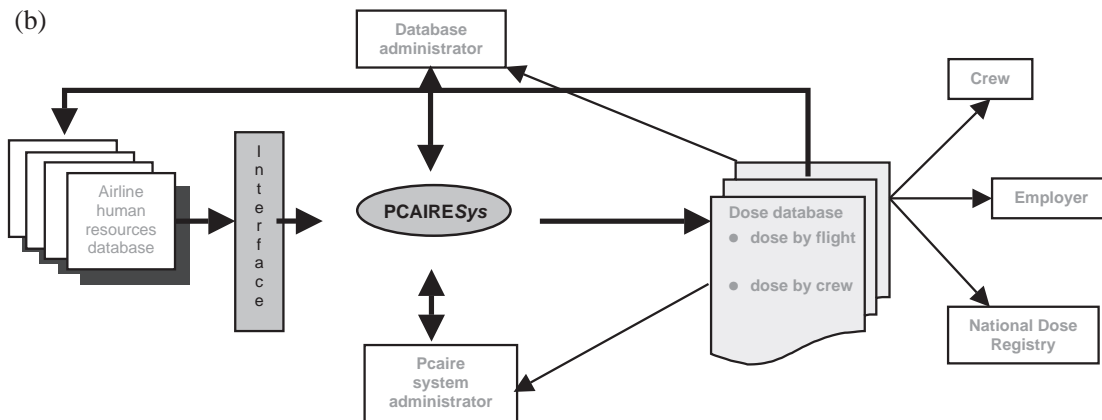


Figure 7. PCAIRE code implementation showing (a) the graphical user interface and (b) operation environment for commercial application.

extrapolation is still required to zero. Thus, these corrections may have led to the slight systematic offset seen near the equator in Figure 6b for the two TEPC curves (i.e. as further compared to the summed instrument curves) where indeed the low-LET component is more predominant. Nevertheless, since all corresponding curves fall within the instrument error (up to ~20%), the f_1 and f_2 curves in Figure 3 for the TEPC are adopted in the following analysis of this section.

PCAIRE code development

Equations 5–11 have been encapsulated into the PCAIRE code, developed in a Visual C++ platform (Figure 7a). The code was written to be user-friendly and requires minimal time for data input, calculation and data storage. The code requires the user to input the date of the flight, the origin and destination airports, the ascent and descent times, and the altitudes and times flown at these altitudes. The user

must select a solar modulation model. A great circle route is produced between the two airports or specific waypoints. From this path information, the geographical position of the aircraft and cut-off rigidity are calculated for every minute of the flight. The at-altitude ambient dose equivalent rate is then integrated along the path at 1 min intervals using the model of Equation 10, which is based on the normalised correlations in Equation 8 (or Figure 3), and unfolded to the actual altitude flown (Equation 5) and the solar modulation potential for the date of the flight. A batch file capability is also offered for an analysis of many flights. The code provides an output of the route dose in units of $H^*(10)$ and effective dose.

As the PCAIRE model is comprised of simple correlations (e.g. Equations 5–11), it can be readily employed as a kernel into an employee flight frequency database as needed for routine application to manage commercial aircrew exposure for a large number of personnel and flights (Figure 7b). As such, a PCAIRE_{sys} code has been developed that is comprised of an underlying kernel model and a wrapper employing the structure queried language (SQL) of ORACLE. This code is therefore capable of providing a secure interface with an airline database so that it can query the crew exposure in terms of such parameters as flight, date, crewmember and occupation. This wrapper also permits data entry in batch mode or with waypoints for routine aircrew exposure assessment.

CODE VALIDATION

A considerable number of jet-altitude flights have been conducted over the past 10 y by several research groups. A validation set of 223 flight measurements has been compiled, including RMC TEPC data obtained from 1998 to 2002 and experimental data by European investigators. Using flight-profile information, the PCAIRE (v. 7.2) code was used to predict the $H^*(10)$ route doses on the given flights in the database, which could be compared against measurements derived from the various research groups^(17,21,22,46,48–51). The PCAIRE simulations were based on great-circle route calculations, and included a comparison of the different solar modulation models of the NASA–JSC (i.e. deceleration parameter) and RMC (i.e. climax count rate). A comparison of PCAIRE predictions to the measured route dose data from other investigators and RMC are shown in Figures 8 and 9, respectively. In general, the PCAIRE predictions are typically in agreement with the measurements from several different research groups to within $\pm 20\%$. The flights in Figures 8 and 9 were conducted over a range of altitudes (up to 12.4 km) during a period in the

solar cycle from 1997 to 2003 and spanned the entire global range of vertical cut-off rigidities (0–16 GV).

The slight systematic underprediction for the Iberia flights in 2001 to South America in Figure 8c is presumably related to the use of the lower dose rate of f_2 in the model based on the Hawk TEPC measurements in Figure 6b (see discussion in Ion chamber and extended range neutron remmeter analysis section). This observation may suggest that the ‘average’ f_1 and f_2 curves in Figure 6b may be more appropriate for adoption in the PCAIRE code.

PREDICTION OF AIRCREW EXPOSURE FROM SEPs

So far, only the GCR exposure has been considered. In light of recent efforts to manage aircrew occupational exposure, there is a need to estimate the variable exposure from SEPs (especially for higher altitude flights). This requirement is relevant considering the sporadic nature of the solar event that may occur within a period of a day or so compared with the more predictable GCR component. For instance, this variable component may be important for the management of pregnant crew members, where lower dose limits apply in order to protect the fetus. Regulations are being developed to limit the additional effective dose to the fetus < 1 mSv during the remainder of the pregnancy⁽⁹⁾.

A model was developed previously to estimate the additional exposure from a solar proton event by correlating the GOES satellite proton flux data with TEPC measurements made on-board the International Space Station (ISS)⁽²²⁾. Unfortunately, the exposure predictions deviated by over $\sim 250\%$ to actual jet altitude measurements because of the large extrapolation distances involved, where increased proton fluxes at geosynchronous orbits ($\sim 30,000$ km) and exposure measurements on the ISS (400 km) do not accurately reflect conditions deep inside the Earth’s atmosphere (at ~ 11 km). Instead, a new model is proposed in this work based on measurements made at altitude as correlated to ground-level neutron monitoring (Figure 10). This model must consider the individual characteristics of the SEP, including its varying intensity and energy spectrum. Consequently, the following dose rate \dot{H}_{SEP} (in $\mu\text{Sv h}^{-1}$) expression is proposed:

$$\dot{H}_{\text{SEP}}(R_c^{\text{eff}}, h, t) = f_{\Delta\%}(t) f_h(h) f_{Rc}(R_c^{\text{eff}}), \quad (12)$$

which must take into consideration the relative intensity of the flare ($f_{\Delta\%}$), as well as the altitude (f_h) and position (f_{Rc}) of the aircraft. The specific function $f_{\Delta\%}$ ⁽⁴³⁾ is developed using the NM at the South Pole by correlating these data with the ambient dose equivalent rate (i.e. subtracting off the GCR contribution) as measured on an aircraft

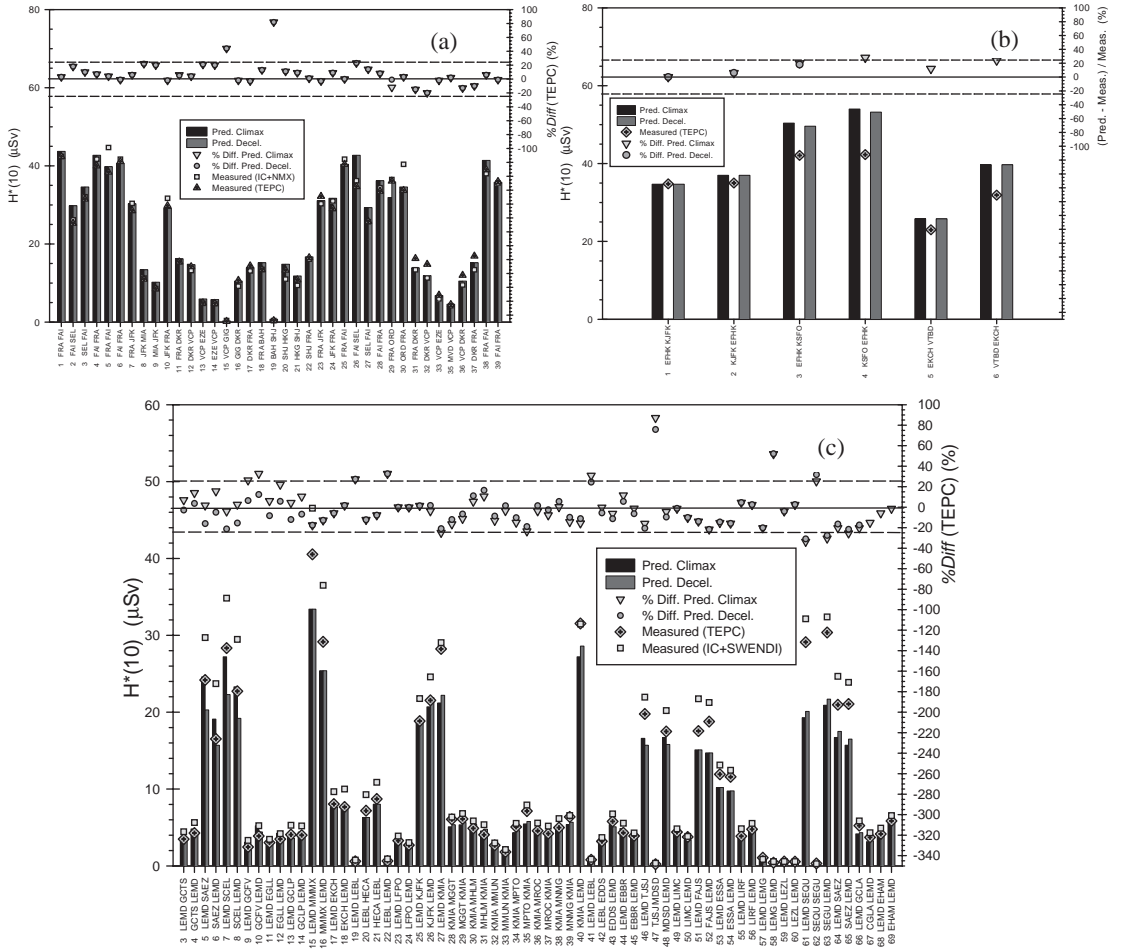


Figure 8. PCAIRE predictions versus integral route dose measurements. (a) Comparison to measurements made by the PTB as part of the ACREM measurement program on 39 flights from May 1997 to February 1999 (during a minimum in the solar cycle)^(17,46). On these flights, an estimate of the ambient dose equivalent was obtained with a TEPC and by the summation of data from an NMx NM and ion chamber (IC). (b) Comparison of PCAIRE predictions to six measurements made by the SSI using another type of TEPC during 1998^(50,51). (c) PCAIRE predictions to 67 Iberia flights from February to September 2001⁽⁴⁹⁾.

by Spurný *et al.* with a MDU LIULIN silicon-based spectrometer. These data were obtained for a ground level event (GLE) 60 on 15 April 2001 for a flight between Prague (PRG) and New York City (JFK)⁽⁵²⁾. As shown in Figure 11, the ambient dose equivalent rate ($f_{\Delta\%}$) (in $\mu\text{Sv h}^{-1}$) can be related to the measured percentage increase ($\Delta\%$) in the neutron count rate at the South Pole monitor (Figure 10) as:

$$f_{\Delta\%} = 1.94 + 0.0265 \times \Delta\%. \quad (13)$$

The South Pole monitor was chosen because of its enhanced sensitivity due to its location at the pole, where the geomagnetic effects are minimal, and its

high altitude (2820 m as opposed to <200 m for most other monitors). This model implicitly assumes that the GLE is isotropic.

Equation 13 can then be used to convert time-dependent ground level counting data at the South Pole NM during a particular (past or future) event, $[\Delta\%(t)]$, into a time-dependent ambient dose equivalent rate for any given flight. The term $f_h = e^{-\xi_{\text{SEP}}(h-h_{\text{SEP}})}$ in Equation 12 is analogous to that in Equation 5 and yields a correction for flights taken at altitudes different from the PRG–JFK reference flight (which occurred at an average atmospheric depth of $h_{\text{SEP}} = 235 \text{ cm}^2 \text{ g}^{-1}$). The parameter $\xi_{\text{SEP}} = 0.0141 \text{ cm}^2 \text{ g}^{-1}$ is a relaxation length for the

ASSESSMENT OF AIRCREW RADIATION EXPOSURE

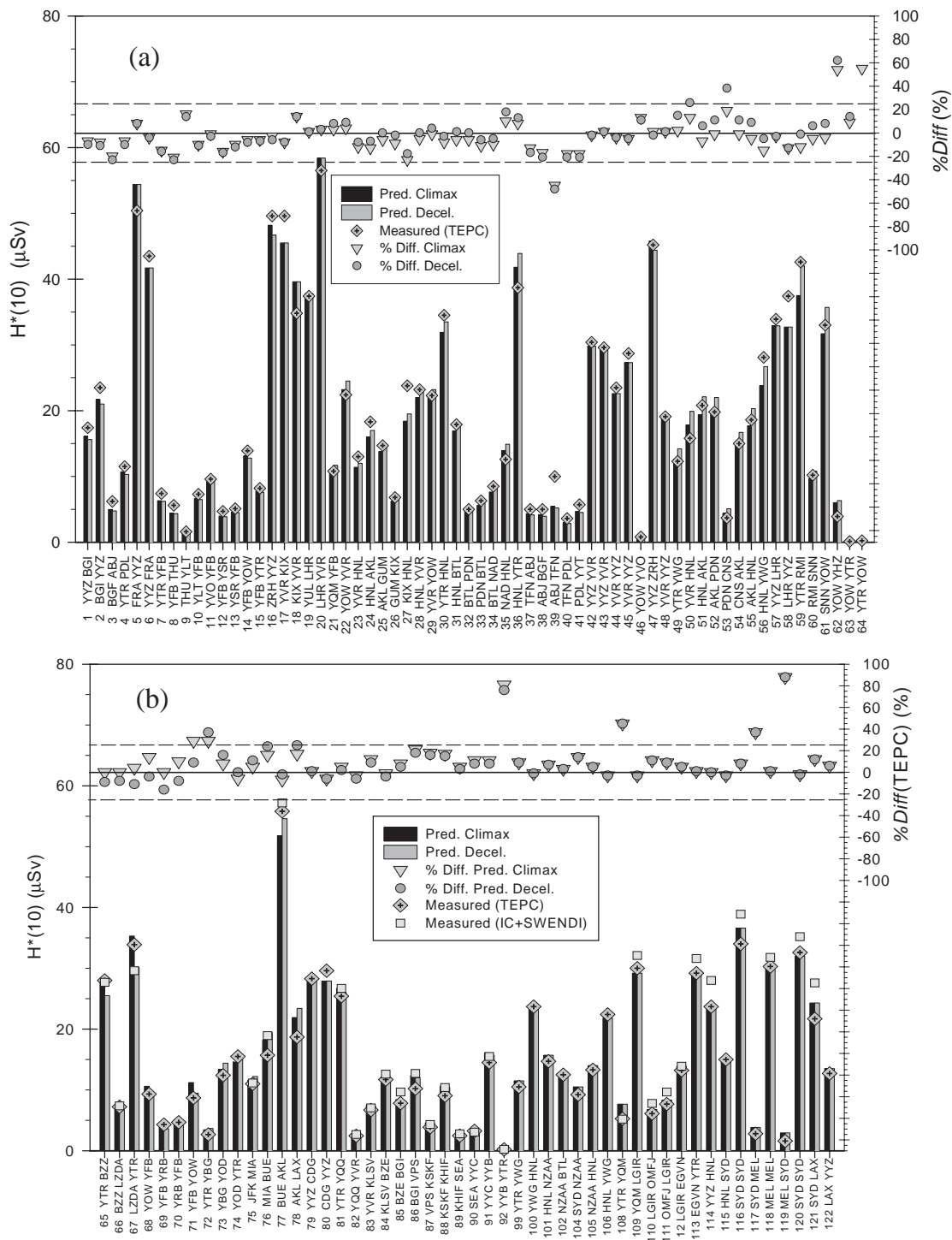


Figure 9. PCAIRE predictions vs. integral route dose measurements by RMC for (a) 64 flight measurements with a TEPC (Original) in 1999 and (b) 50 flight measurements with a TEPC (Hawk) and summed SWENDI + IC data in 2001–2003⁽⁴⁸⁾.

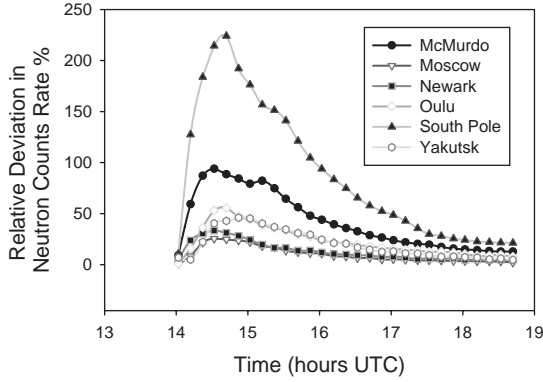


Figure 10. Relative neutron count deviation curves for various monitoring stations during GLE 60.

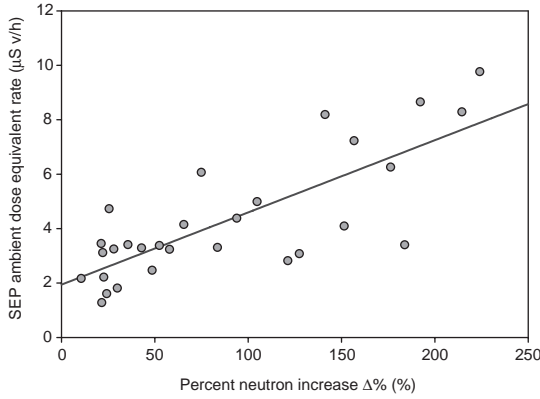


Figure 11. PRG-JFK flight SEP dose rate vs. South Pole NM percentage neutron increase. The linear regression line is given by Equation 13.

attenuation of the SEP ambient dose equivalent rate in the atmosphere, which is estimated with a FREE transport code calculation^(22,53).

The function f_{Rc} takes into consideration the given flight path, which depends on the effective cut-off rigidity R_c^{eff} , and reflects the individual nature of the particle-energy spectrum (i.e. the ability for particles to penetrate through the geomagnetic shield). This function is derived from ground-level neutron counting data (as a post-event analysis) using the peak of the percentage difference values for various stations (see, e.g., Figure 10)^(43,54). This approach conservatively assumes that there is no softening of the energy spectrum during the late phase of the GLE. The f_{Rc} function is normalised so as to provide a value of unity at the average R_c^{eff} value (1.24 GV) for the given reference flight (Figure 12a):

$$f_{Rc} = 1.61 - 0.493 \times R_c^{\text{eff}}. \quad (14)$$

Note that $f_{Rc} = 0$ for locations with R_c^{eff} values above ~ 3.3 GV in Figure 12a and, therefore, no additional SEP exposure would be expected for latitudes below this value where adequate shielding is provided by the Earth's magnetic field. As each solar radiation event is unique, the effect of latitude for an individual event can be accounted for with a similar (post-event) analysis (e.g. compare Figures 12a and b for GLE 60 and GLE 42, respectively).

Finally, magnetic storms can affect the magnetic field lines of the Earth (and hence the vertical cut-off rigidity)⁽⁵⁵⁾. This effect can be modelled further by impressing a uniform magnetic field for the storm on the normal quiet field using an effective cut-off rigidity R_c^{eff} as given in Equation 13 of Ref. (22) (where the storm field is characterised by a global average K_p index)⁽⁵⁶⁾. Alternatively, a magnetospheric geomagnetic cut-off rigidity model is available by Smart and Shea (RCINTUT6)^(57,58). This model is based on the IGRF95 internal quiescent geomagnetic field with the Tsyganenko magnetospheric model included for the effects of magnetic activity (via a K_p index) and the daily variation introduced by the Earth's rotation.

Recent data obtained with two measurement flights, as part of the DOSMAX project, during GLE 60 (15 April 2001), can be used to test and validate the SEP-exposure model⁽¹⁹⁾. The implementation of the model can be first tested for consistency against the MDU-LIULIN data that was used to develop the correlation in Figure 11, i.e. for the PRG-JFK flight as shown in Figure 13a. Thus, using Equations 12–14 and the $\Delta\%$ data for the South Pole NM as a function of time t in Figure 10, an integrated SEP ambient dose equivalent of 20.5 ± 8.2 μSv was predicted. As expected, this predicted value compared well to a measurement of 20.7 ± 7.9 μSv for the flight. The SEP contribution was determined by subtracting the GCR contribution (using PCAIRE V7.2) from the total measurements over the event period.

The ACREM group obtained additional exposure data using a G-M tube on-board a second jet-altitude flight between Frankfurt (FRA) and Dallas (DFW)⁽¹⁹⁾. These data were scaled using LUN transport calculations to provide ambient dose equivalent rates as given in Figure 13b throughout the event. Using again the model in Equations 12–14, with the South Pole data in Figure 10, the ambient dose equivalent rate can be predicted and subsequently validated against the independent ACREM data for a different flight route. It can be seen in Figure 13b that the model reproduces both the shape and timing of the dose rate curve quite well. Furthermore, integrating Equation 12 with a time step size of 15 min, the model predicts an accumulated ambient dose equivalent of ~ 21 μSv for this solar flare event. A PCAIRE estimation of the

ASSESSMENT OF AIRCREW RADIATION EXPOSURE

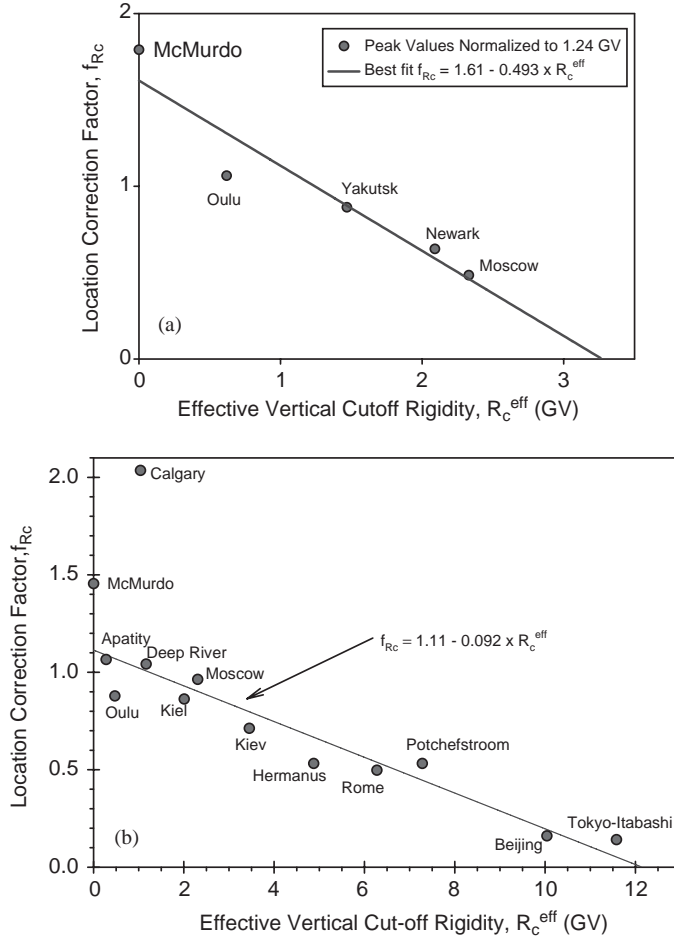


Figure 12. Weighting function f_{Rc} for (a) GLE 60 and (b) GLE 42.

galactic exposure for the flight was $38 \mu\text{Sv}$, i.e. the solar particle exposure for this route was approximately half that of the galactic radiation exposure. Consequently, for GLE 60, the total aircrew radiation exposure was predicted to be $59 \mu\text{Sv}$. By comparison, the accumulated dose with ACREM was $\sim 60 \mu\text{Sv}$ (which also included the galactic contribution)⁽¹⁹⁾. This excellent agreement suggests that the simple proposed empirical model may be able to predict SEP contributions for future GLEs using ground-level data for the event.

In the proposed SEP model, a simple function f_{Rc} was used to correct for the effect of latitude; however, longitudinal variations can also arise as the solar wind wraps around the Earth and interacts with the geomagnetic field. This is especially true for the relativistic protons that give rise to a very localised effect, as demonstrated in Figure 14 with a comparison of the Goose Bay and Apatity neutron

monitor data during GLE 42 (despite the fact that both monitor locations have a similar cut-off rigidity). The relativistic protons give rise to the observed discrepancy in the early part of the event since they are the first to reach the Earth; however, the radiation levels become quite similar with increasing time as the event proceeds.

It has been suggested that the protons are more penetrating in the 14–16 Magnetic Local Time (MLT) region (i.e. in the early afternoon at the given local time)⁽⁵⁹⁾. However, a review of neutron monitoring data during GLE 39–60 (Table 3) suggests that most enhancements actually occur in the early morning (i.e. at ~ 6 MLT)⁽⁶⁰⁾. Because this result does not always occur, longitudinal effects were not considered in the current model. However, the impact of ignoring this effect can be estimated by comparing several neutron monitor readings during GLE 42 (which is the second largest event ever

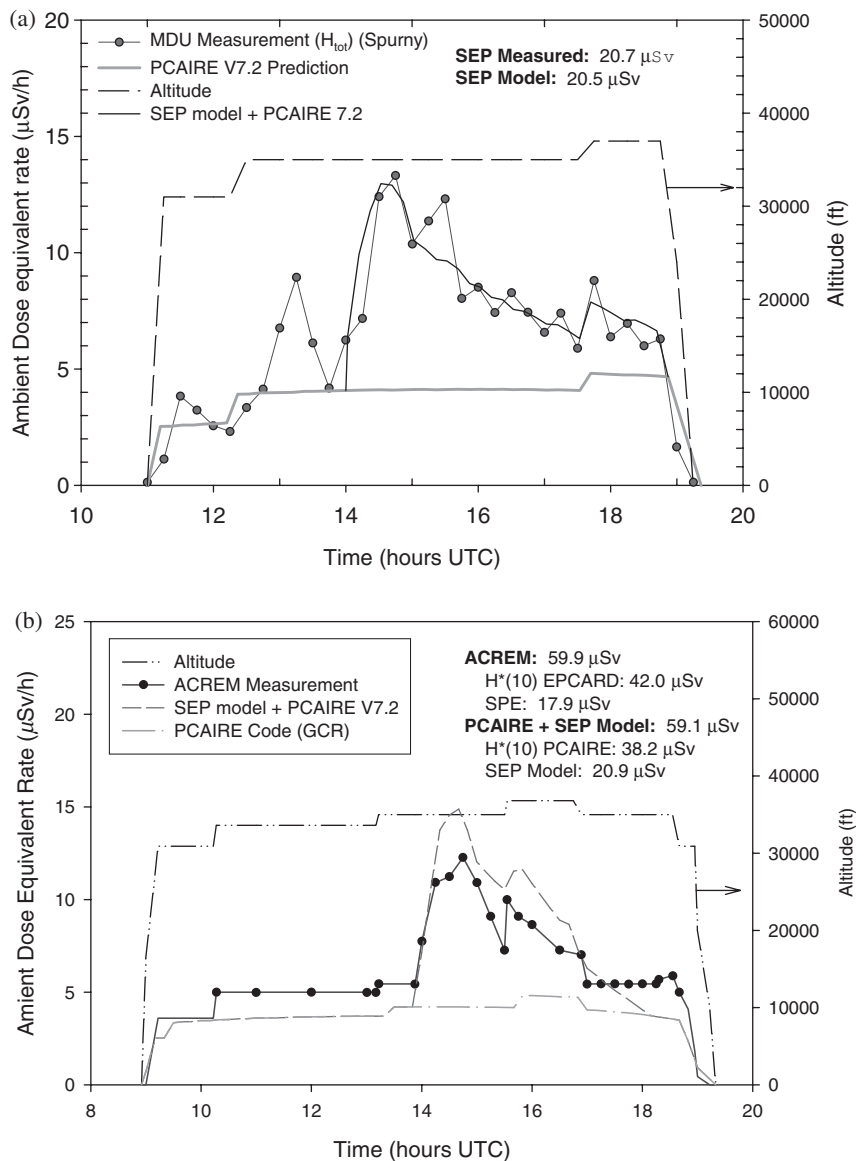


Figure 13. Comparison of SEP model prediction to (a) the MDU-LIULIN measurement for the reference flight, PRG-JFK and (b) ACREM measurement for the validation flight, FRA-DFW.

recorded). For instance, as shown in Table 3, the Calgary monitor indicated a maximum ~400 percentage increase, which was significantly larger than any other location, including the Deep River monitor (which had a similar cut-off rigidity value) (Figure 12b)⁽⁶¹⁾. Utilising the data in Figure 12b for the Calgary monitor (instead of the Deep River one) in the model would result in an increased SEP exposure prediction by ~55%. This calculation therefore

provides an upper-bound error that could result if longitudinal effects are ignored.

MODEL APPLICATION

The current models developed in the Model development and Prediction of aircrew exposure from SEPs sections can be used to provide estimates of the annual and career exposures of aircrew as a

ASSESSMENT OF AIRCREW RADIATION EXPOSURE

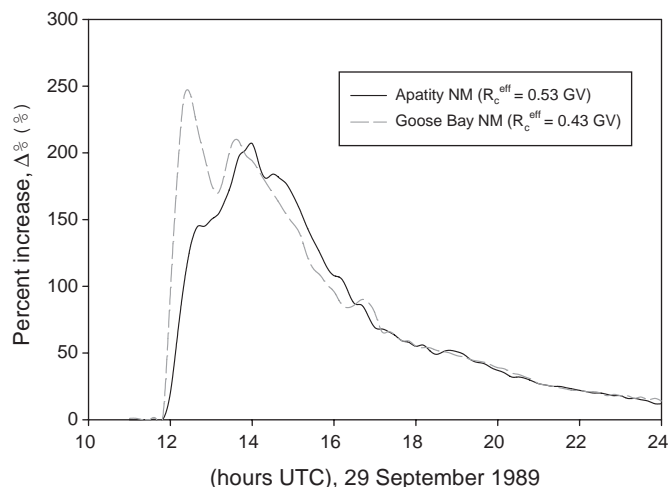


Figure 14. Comparison of two neutron monitors at similar cut-off rigidities during GLE 42 (29 September 1989).

Table 3. MLT regions of interest for various GLEs*.

GLE	Date	$\Delta\%$ _{South Pole NM}	'Notable' NM**	$\Delta\%$	MLT region
39	16-Feb-84	212	Goose Bay	98	6-8
41	16-Aug-89	15	Mawson	18	4-6
42	29-Sep-89	365	Calgary	403	4-6
			Inuvik	377	2-4
			Thule	374	6-8
			Cape Schmidt	355	0-2
43	21-Oct-89	92	None	—	—
44	22-Oct-89	101	McMurdo	193	4-6
45	24-Oct-89	205	McMurdo	111	6-8
46	15-Nov-89	5	Thule	6	2-4
			Kiev	6	8-10
47	21-May-90	15	Thule	24	16-18
48	24-May-90	37	Calgary	36	12-14
49	26-May-90	13	Thule	10	16-18
50	27-May-90	12	Kiev	8	2-4
51	11-Jun-91	14	Moscow	13	4-6
52	15-Jun-91	57	None	—	—
53	25-Jun-92	5	Tixie Bay	7	4-6
54	2-Nov-92	N/A	None	—	—
55	6-Nov-97	N/A	Mawson	15	16-18
59	14-Jul-00	59	Thule	46	4-6
60	15-Apr-01	243	McMurdo	109	0-2

N/A, not available

*Data obtained from GLE database at Ref. (61)

***'Notable' indicates stations that displayed an unusually high $\Delta\%$ as compared with other neutron monitors with a similar cutoff rigidity location ($R_c \sim 0$ GV for Thule, McMurdo, Inuvik and Cape Schmidt NMs)

result of GCR and SEP contributions by considering actual flight histories of aircrew⁽¹⁵⁾. For instance, in the current analysis, the actual flight history for a pilot during 1997, who had participated in an RMC study with neutron bubble detectors (99 flights with 682 h accrued), was extrapolated over a 30-y period (from 1973 to

2002). This calculation takes into consideration the actual changing (time-dependent) solar modulation conditions as well as the two most predominant solar particle events that had occurred during this 30-y period (i.e. GLE 42 on 29 September 1989 and GLE 60 on 15 April 2001) (Table 3). In fact, the former event is the largest solar event ever

recorded since 1956. A higher altitude of 13.0 km was further assumed for the 1989 flight as a 'worst case' exposure situation during a typical commercial flight.

Table 4. Career dose estimate.

	GCR (mSv)	SEP (mSv)	Total (mSv)
Career GCR	89.0 ± 17.8	—	89.0 ± 17.8
SEP (GLE 42)	0.054 ± 0.011	0.159 ± 0.064	0.213 ± 0.065
SEP (GLE 60)	0.032 ± 0.006	0.021 ± 0.008	0.052 ± 0.010
Career dose	~89.1 (99.8%)*	~0.2 (0.2%)*	~89.3

*The number in the parentheses represents the percentage of the total career dose

The annual (GCR) doses varied with changing solar modulation (from 2.4 to 3.3 mSv y⁻¹), in accordance with the 40% solar cycle variation (Solar modulation and latitude effects section). The PCAIRE code prediction for 1997 was 3.3 mSv, which was within ~8% of that estimated from cumulative (scaled) bubble detector measurements⁽¹⁵⁾. Overall, this analysis predicted a career GCR exposure of 89 mSv, as compared to only 0.2 mSv for the two SEPs (Table 4). Thus, the GCR contribution is much more significant and makes up 99.8% of the career dose. On the other hand, the SEP dose contribution can be an important factor for pregnant flight crew where, as shown in Figure 15a, it contributes to nearly three quarters of the total route dose during the single flight (compared with just 6% of the annual exposure as shown in Figure 15b).

As shown in Figure 16, the cruising altitude is a more important factor for the SEP contribution to the route dose than that for the GCR contribution.

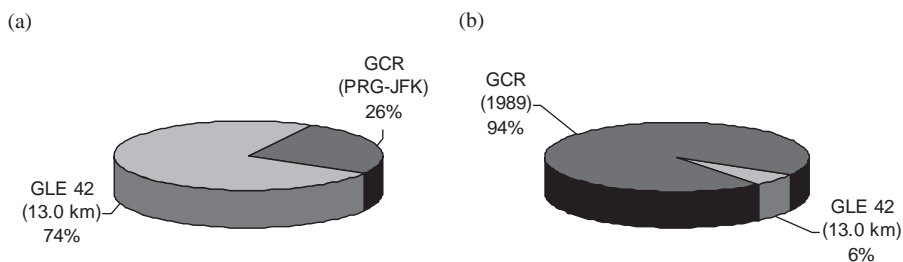


Figure 15. Comparative dose contributions for the SEP (for GLE 42) and GCR components: (a) during the single PRG-JFK flight (29 September 1989); and (b) for the entire year (1989).

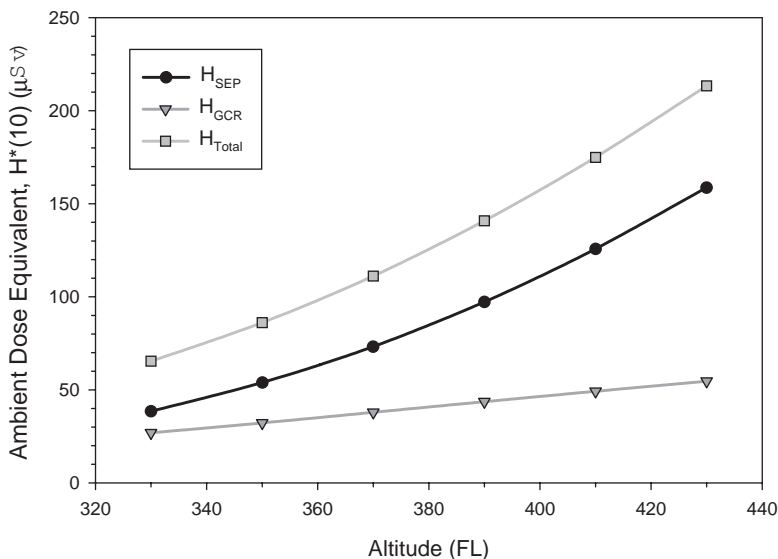


Figure 16. GCR and SEP exposures for flight PRG-JFK during GLE 42 from 10.0 km (FL 330) to 13.0 km (FL 430).

This result occurs because the SEP relaxation length for the atmosphere (ξ_{SEP}) is about two times that for the GCR (ξ_{GCR}) due to the fact that primary SEP protons have a much lower energy spectrum as compared to that of the primary GCRs. Moreover, the GLE 42 event was significantly more penetrating as compared with GLE 60 as indicated by the ground-level neutron monitoring data, where increased readings were detected at much lower latitudes (compare Figures 12a and b).

CONCLUSIONS

- (1) A TEPC, supported by other equipment in a measurement suite, was utilised further to conduct an extensive series of in-flight measurements on 122 flights to investigate aircrew radiation exposure at jet aircraft altitudes over the solar cycle (9.4–12.4 km). These data have been used to develop further the semi-empirical model, previously incorporated into the PCAIRE computer code, for the prediction of aircrew exposure to galactic cosmic radiation on any given flight. This code was used to generate predictions of route dose exposures for approximately 200 flights on which measured data were also available. On most flights, the code agreed with the measured data (within about $\pm 20\%$). A model has also been developed to predict the exposure levels from solar flares at jet altitudes utilising available ground-level neutron monitoring data. This work further proves that the PCAIRE code can be used with confidence for estimating aircrew exposure by air carriers in meeting regulatory requirements.
- (2) The semi-empirical models have been applied to predict the annual exposure (e.g. a GCR exposure of 3.3 mSv for 99 flights with 682 h accrued in 1997) and career exposure (e.g. 89.3 mSv from GCR and SEP exposure over 1973–2002) of a flight crew member using actual flight history and solar modulation data. The continual GCR contribution is predominant at commercial jet altitudes and makes up $\sim 99.8\%$ of the career dose as compared with the sporadic exposure that arises from several solar particle enhancements (e.g. GLE 42 and 60). On the other hand, the SEP dose contribution can be an important factor for pregnant flight crew where, for instance, it can be comparable to the GCR exposure as acquired over a single flight.

ACKNOWLEDGEMENTS

The authors would like to thank J.D. Servant (Transport Canada), and Dr S. Kupca and C.J. Thorp (Director General Nuclear Safety), for their assistance, support and guidance in this study. The

authors would further like to express their gratitude to Air Canada, Air France, British Airways, Qantas and Iberia for their assistance and cooperation in the arrangement for measurements on commercial flights. The authors express their appreciation to 1 Canadian Air Division of the Canadian Forces, Air Operations and members of the 437 Transport Squadron at 8 Wing Trenton for their assistance and cooperation on the military flights. Finally, the authors would like to acknowledge and thank U. Schrewe (PTB/Hannover University) for the use of the TEPC and IC+NMX data, F. Spurný (CAS) for the Liulin data during GLE 60. The authors would also like to thank P. Beck (ACRS) for many helpful discussions on TEPC calibration. The neutron monitors of the Bartol Research Institute are supported by a NSF grant ATM-0000315. Financial support for this study was provided by Transport Canada and DGNS.

REFERENCES

1. Gaisser, T. K. *Cosmic Rays and Particle Physics* (Cambridge: Cambridge University Press) (1990).
2. Heinrich, W., Roesler, S. and Schraube, H. *Physics of cosmic radiation fields*. Radiat. Prot. Dosim. **86**(4), 253–258 (1999).
3. O'Brien, K. and Sauer, H. H. *On the atmospheric response to solar-particle events*. Int. J. Geomagnet. Aeronomy **2**(3), 181–188 (2001).
4. Reames, D. V. *Solar energetic particle variations*. Adv. Space Res. (in press).
5. International Commission on Radiological Protection. *1990 Recommendations of the International Commission on Radiological Protection*. ICRP Publication 60. Ann. ICRP **21**(1–3) (Oxford: Pergamon Press) (1991).
6. Courades, J.-M. *European legislation on protection against cosmic radiation*. Radiat. Prot. Dosim. **86**(4), 7–24 (1999).
7. Council Directive 96/29/EURATOM of 13 May 1996 laying down basic safety standards for the protection of the health of workers and the general public against the dangers arising from ionising radiation. Off. J. Eur. Commun. **39**(L159), (1996).
8. European Commission. *Recommendations for the implementation of Title VII of the Basic Safety Standards Directive (BSSD) concerning significant increase in exposure due to natural radiation sources*. European Commission Radiation Protection Report 88 (1996), ISBN 92-827-5336-0.
9. Transport Canada. *Measures for managing exposure to cosmic radiation of employees working on board aircraft*. Commercial and Business Aviation Advisory Circular No. 0183 (2001), Available on http://www.tc.gc.ca/aviation/commerce/advisory/english/ac0183_e.htm.
10. International Commission on Radiological Protection. *General principles for the radiation protection of workers*. ICRP Publication 75. Ann. ICRP **27**(1) (Oxford: Pergamon Press) (1997).

11. van Dijk, J. W. E. *Dose assessment of aircraft crew in the netherlands*. Radiat. Prot. Dosim. **106**(1), 25–32 (2003).
12. Reitz, G. *Radiation environment in the Stratosphere*. Radiat. Prot. Dosim. **48**, 5–20 (1993).
13. Beck, P., Ambrosi, P., Schrewe, U. and O'Brien, K. *ACREM: Air Crew Radiation Exposure Monitoring*. 4th European Commission Framework Program, Contract FI4P-CT96-0047, Report No. OEFZS-G-0008, ARCS, Seibersdorf, November (1999).
14. Schrewe, U. J. *Radiation exposure monitoring in civil aircraft*. Nucl. Instrum. Meth. A422, 621–625 (1999).
15. Lewis, B. J., Tume, P., Bennett, L. G. I., Pierre, M., Green, A. R., Cousins, T., Hoffarth, B. E., Jones, T. A. and Brisson, J. R. *Cosmic radiation exposure on canadian-based commercial airline routes*. Radiat. Prot. Dosim. **86**(1), 7–24 (1999).
16. Beck, P., Bartlett, D., O'Brien, K. and Schrewe, U. *In-flight validation and routine measurements*. Radiat. Prot. Dosim. **86**, 303–308 (1999).
17. Schrewe, U. J. *Global measurements of the radiation exposure of civil air crew from 1997 to 1999*. Radiat. Prot. Dosim. **91**(4), 347–364 (2000).
18. Goldhagen, P. *Overview of aircraft radiation exposure and recent ER-2 measurements*. Health Phys. **79**, 526–544 (2000).
19. Bartlett, D. T. and others. *Investigation of radiation doses at aircraft altitudes during a complete solar cycle*. In: SOLSPSA Space Weather Workshop, Vico Equense, Italy, 25–29 September (2001).
20. Saez, Vergara, J. C., Gutiérrez, A. M. R., Jiménez, R. R., Román, R. D.-M., Garcia, P. O. and Merelo de Barberá, F. *Monitoring of the cosmic radiation at Iberia commercial flights: one year experience of in-flight measurements*. In: 12th Biennial Topical Meeting of the Radiation Protection and Shielding Division of the American Nuclear Society, Doses in Aircraft Session, Sante Fe, AZ, 14–18 April (2002).
21. Lewis, B. J., McCall, M. J., Green, A. R., Bennett, L. G. I., Pierre, M., Schrewe, U. J., O'Brien, K. and Felsberger, E. *Aircrew exposure from cosmic radiation on commercial airline flights*. Radiat. Prot. Dosim. **93**(4), 293–314 (2001).
22. Lewis, B. J., Bennett, L. G. I., Green, A. R., McCall, M. J., Ellaschuk, B., Butler, A. and Pierre, M. *Galactic and solar radiation exposure to aircrew during a solar cycle*. Radiat. Prot. Dosim. **102**(3), 207–227 (2002).
23. Taylor, G. C., Bentley, R. D., Conroy, T. J., Hunter, R., Jones, J. B. L., Pond, A. and Thomas, D. J. *The evaluation and use of a portable TEPC system for measuring in-flight exposure to cosmic radiation*. Radiat. Prot. Dosim. **99**(1–4), 435–438 (2002).
24. Roesler, S., Heinrich, W. and Schraube, H. *Calculation of radiation fields in the atmosphere and comparison to experimental data*. Radiat. Res. **149**, 87–97 (1998).
25. Ferrari, A., Pelliccioni, M. and Rancati, T. *Calculation of the radiation environment caused by galactic cosmic rays for determining air crew exposure*. Radiat. Prot. Dosim. **93**(2), 101–114 (2001).
26. Roesler, S., Heinrich, W. and Schraube, H. *Monte Carlo calculation of the radiation field at aircraft altitudes*. Radiat. Prot. Dosim. **98**(4), 367–388 (2002).
27. Schraube, H., Leuthold, G., Heinrich, W., Roesler, S., Mares, V. and Schraube, G. *EPCARD (European Program Package for the Calculation of Aviation Route Doses)*. User's Manual, GSF National Research Centre for Environment and Health (2002).
28. O'Brien, K., Friedberg, W., Sauer, H. S. and Smart, D. F. *Atmospheric cosmic rays and solar energetic particles at aircraft altitudes*. Environ. Int. **22**(Suppl. 1), S9–S44 (1996).
29. O'Brien, K. *LUIN, a code for the calculation of cosmic ray propagation in the atmosphere*. Update of HASL-275, EML-338 (1978).
30. CARI-6 (computer program). Oklahoma City, OK, Federal Aviation Administration, Civil Aeromedical Institute. Available on <http://www.cami.jccbi.gov/AAM-600/Radiation/600radio.html>.
31. Green, A. R., Lewis, B. J., Bennett, L. G. I., McCall, M. J. and Ellaschuk, B. *Cosmic radiation exposure of aircrew—phase II, volume 1: visual PC-AIRE theory manual and volume 2: visual PC-AIRE user's manual*. Project Report to Transport Canada, March (2001).
32. Kellerer, A. M. and Hahn, K. *Considerations on a revision of the quality factor*. Radiat. Res. **114**, 480–488 (1988).
33. International Commission on Radiation Units and Measurements. *The quality factor in radiation protection*. ICRU Publication 40 (Bethesda, MD: ICRU) (1986).
34. Osler, R. H., Hsu, H.-H., Beverding, A., Kleck, J. H., Casson, W. H., Vasilik, D. G. and Devine, R. T. *WENDI: an improved neutron remmeter*. Los Alamos National Laboratory Report LA-UR-99-6551. Health Phys. **79**(2), 170–181 (2000).
35. International Commission on Radiological Protection. *Conversion coefficients for use in radiological protection against external radiation*. ICRP Publication 74. Ann. ICRP **26**(3/4), Oxford: Pergamon Press (1996).
36. Roesler, S. Private communication, CERN, November (2000).
37. Ellaschuk, B. *Assessment of Canadian forces aircrew exposure to cosmic radiation*. M. Eng. Thesis, Royal Military College of Canada, May (2001).
38. O'Brien, K. and Burke, G. de P. *Calculated cosmic neutron monitor response to solar modulation of galactic cosmic rays*. J. Geophys. Res. **78**, 3013 (1973).
39. Wilson, M. Bartol Research Institute and Vashenyuk, E. Polar Geophysical Institute, Russia, Available in <http://www.cami.jccbi.gov/AAM-600/Radiation/600radio.html>.
40. Badhwar, G. D. *The radiation environment in low-earth orbit*. Radiat. Res. **148**, 3–10 (1997).
41. O'Brien, K. Private communication, Northern Arizona University, 2 July (2003).
42. NOAA. Available on www.sec.noaa.gov/ftpdir/plots/2003_plots/proton/20030531_proton.gif, 3 June (2003).
43. Bartol Research Institute. Available on www.bartol.udel.edu/~neutronm/realtime/inuvik.html, 3 June (2003).
44. Available on ulysses.sr.unh.edu/NeutronMonitor/Misc/neutron2.html
45. Available on ftp.ngdc.noaa.gov/STP/SOLAR_DATA/COSMIC_RAYS/CLIMAX.TAB.
46. Schrewe, U. J. *ACREM—Air Crew Radiation Exposure Monitoring: results from the in-flight measurement program of the PTB: summary of the radiation monitoring data PTB-6.31-1999-1*, Physikalisch Technische

ASSESSMENT OF AIRCREW RADIATION EXPOSURE

- Bundesanstalt, Braunschweig, Germany, August (1999).
47. Autischer, M., Beck, P., Ferrari, A., Pelliccioni, M. and Rollet, S. *Dosimetric considerations on TEPC FLUKA-Simulation and measurements*. In: 9th Neutron Dosimetry Symposium, Advances in Nuclear Particle Dosimetry for Radiation Protection and Medicine, Delft University of Technology, The Netherlands, September 28–October 3 (2003).
 48. Desormeaux, M. *Galactic and solar radiation exposure of aircrew over a solar cycle*. M.A.Sc. Thesis, Royal Military College of Canada, October (2003).
 49. Saez-Vergara, J. C. *CIEMAT, Servicio de Protección Radiológica*, Private communication (2003).
 50. European Commission. *Study of radiation fields and dosimetry at aviation altitudes*. Final Report for European Commission Contract F14P-CT950011, Coordinated by the Dublin Institute for Advanced Studies, School of Cosmic Physics, Dublin, Ireland, Report 99-9-1 (1999).
 51. Kyllonen, J.-E., Lindborg, L. and Samuelson, G. *Cosmic radiation measurements on-board aircraft with the variance method*. *Radiat. Prot. Dosim.* **93**, 197–205 (2001).
 52. Spurný, F. and Dachev, T. *Intense solar flare measurements, April 15 2001, Letter to the Editor*, *Radiat. Prot. Dosim.* **95**, 273–275 (2001).
 53. Felsberger, E. Private communication, Technical University Graz, May (2001).
 54. Moscow Neutron Monitor Data. Available on <http://helios.izmiran.rssi.ru/cosray/GLE60/c060mosc.txt>.
 55. Dyer, C. S., Lei, F., Clucas, S. N., Smart, D. F. and Shea, M. A. *Calculations and observations of solar particle enhancements to the radiation environment at aircraft altitudes*. *Adv. Space. Res.* **32**(1), 81–93 (2003).
 56. Wilson, J. W., Townsend, L. W., Schimmerling, W., Khandelwal, G. S., Khan, F., Nealy, J. E., Cucinotta, F. A., Simonsen, L. C., Shinn, J. L. and Norbury, J. W. *Transport methods and interactions for space radiations*. NASA Reference Publication 1257, December (1991).
 57. Smart, D. F. and Shea, M. A. *The space-developed dynamic vertical cut off rigidity model and its applicability to aircraft radiation dose*. *Adv. Space. Res.* **32**(1), 103–108 (2003).
 58. User's Manual Version 2. Air Force Research Laboratory, Space Vehicles Directorate, Hanscom AFB, MA 01731 (to be released).
 59. Vashenyuk, E. V., Gvozdevsky, B. B., Usoskin, I. G., Mursula, K. and Kovaltsov, G. A. *The ground-level enhancement of 14 July 2000: explaining the difference between near-by neutron monitors at apatity and Oulu*. In: Proceedings of ICRC 2001, Copernicus Gesellschaft, pp. 3383–3386 (2001).
 60. Smart and Shea. Private communication, 2002.
 61. GLE database. Australian Antarctic Data Centre, Government of Australia, May (2003), Available on aadc-maps.aad.gov.au/aadc/gle/.